



## Get Clarity On Generics

Cost-Effective CT & MRI Contrast Agents



FRESENIUS  
KABI

WATCH VIDEO

# AJNR

## **MRI Posttreatment Surveillance for Head and Neck Squamous Cell Carcinoma: Proposed MR NI-RADS Criteria**

M.M. Ashour, E.A.F. Darwish, R.M. Fahiem and T.T. Abdelaziz

This information is current as of August 4, 2025.

*AJNR Am J Neuroradiol* published online 11 March 2021  
<http://www.ajnr.org/content/early/2021/03/11/ajnr.A7058>

# MRI Posttreatment Surveillance for Head and Neck Squamous Cell Carcinoma: Proposed MR NI-RADS Criteria

 M.M. Ashour,  E.A.F. Darwish,  R.M. Fahiem, and  T.T. Abdelaziz

## ABSTRACT

**BACKGROUND AND PURPOSE:** The current Neck Imaging Reporting and Data System (NI-RADS) criteria were designed for contrast-enhanced CT with or without PET. Prior studies have revealed the capability of DWI and T2 signal intensity in distinguishing locoregional tumor residual and recurrence from posttreatment benign findings in head and neck cancers. We aimed to propose MR imaging NI-RADS criteria by adding diffusion criteria and T2 signal intensity to the American College of Radiology NI-RADS template.

**MATERIALS AND METHODS:** This retrospective study included 69 patients with head and neck squamous cell carcinoma (HNSCC) who underwent posttreatment contrast-enhanced MRI imaging surveillance using a 1.5T scanner. The scans were interpreted by 2 neuroradiologists. Image analysis assessed the primary tumor site using the current American College of Radiology NI-RADS morphologic lexicon (mainly designed for contrast-enhanced CT with or without PET). NI-RADS rescoring was then performed based on our proposed criteria using T2 signal and diffusion features. The reference standard was a defined set of criteria, including clinical and imaging follow-up and pathologic assessment.

**RESULTS:** Imaging assessment of treated HNSCC at the primary tumor site using T2 signal intensity and diffusion features as modifying rules to NI-RADS showed higher sensitivity, specificity, positive predictive value, negative predictive value, and accuracy (92.3%, 90.7%, 85.7%, 95.1%, and 91.3%, respectively) compared with the current NI-RADS lexicon alone (84.6%, 81.4%, 73.3%, 89.8%, and 82.6%, respectively).

**CONCLUSIONS:** The addition of diffusion features and T2 signal to the American College of Radiology NI-RADS criteria for the primary tumor site enhances the specificity, sensitivity, positive predictive value, negative predictive value, and NI-RADS accuracy.

**ABBREVIATIONS:** ACR = American College of Radiology; LTR = locoregional tumor residual or recurrence; NI-RADS = Neck Imaging Reporting and Data System; NPV = negative predictive value; PPV = positive predictive value; SI = signal intensity; CECT = contrast-enhanced CT; CEMRI = contrast-enhanced MRI; HNSCC = head and neck squamous cell carcinoma; RTH = radiation therapy; CRTH = chemoradiation therapy; FP = false-positive; FN = false-negative

The Neck Imaging Reporting and Data System (NI-RADS) was recently introduced by the American College of Radiology (ACR) to precisely convey the level of radiologic suspicion regarding the existence of a recurrent or residual disease.<sup>1,2</sup> Initial studies showed high performance of the NI-RADS system.<sup>3,4</sup> NI-RADS criteria and risk categories were developed for contrast-enhanced CT (CECT) imaging with or without PET for posttreatment neck imaging. Later, these risk categories were applied to contrast-enhanced MRI (CEMRI).<sup>1,2,5</sup> However, there is still no published ACR NI-RADS lexicon for MR imaging surveillance.

Although not included in the NI-RADS scoring system, several studies have revealed the usefulness of DWI and signal intensity on T2WI in identifying residual and recurrent tumors in patients with treated head and neck cancer.<sup>6-9</sup> Based on previous studies, tissues with diffusion facilitation and either low T2 signal intensity (SI) (less than or equal to muscles) that usually represents fibrotic tissue or high T2 SI (approaching the CSF signal), which usually represents edema and granulation, have no to low-level suspicion for malignancy.<sup>6,8</sup> Studies examining the effectiveness of DWI in detecting locoregional tumor residual or recurrence (LTR) in the posttreatment neck consider that the histopathologic features of malignant tissues, such as increased cellularity and nuclear hyperchromatism, result in a diminution of intra- and extracellular spaces available for the diffusion of water protons with a consequent decrease in ADC values. This contrasts with the low cellularity with an increase in interstitial water associated with edema and inflammation, causing subsequent elevation of ADC values.<sup>7,10,11</sup>

Received June 28, 2020; accepted after revision December 20.

From the Department of Diagnostic Radiology, Faculty of Medicine, Ain Shams University, Cairo, Egypt.

Please address correspondence to Manar M. Ashour, MD, Department of Diagnostic Radiology, Faculty of Medicine, Ain Shams University, 38 Ramsis street, Abbassia Square, PO Box 11381, Cairo, Egypt; e-mail: manar.ashour@gmail.com; @manarmaamoun

<http://dx.doi.org/10.3174/ajnr.A7058>

We hypothesized that tailoring NI-RADS criteria for MR imaging with DWI features and T2 SI may improve the diagnostic performance of the existing NI-RADS system for MR imaging surveillance.

This study aimed to recommend new NI-RADS criteria for MR imaging surveillance based on the current system using DWI and T2 signals and to evaluate the diagnostic performance of integrating these criteria into the existing NI-RADS algorithm.

## MATERIALS AND METHODS

### Study Design and Patient Selection

Our institution's ethics committee approved this single-center, retrospective study and waived the requirement for informed consent. Data were retrieved from the medical records and PACS. This study included 69 patients with head and neck squamous cell carcinoma (HNSCC) who were referred for posttreatment MR imaging surveillance between June 2018 and September 2020. Patients with histopathologically diagnosed primary HNSCC who underwent CEMRI surveillance within the first year after treatment, starting from 8–10 weeks after completing their treatment course, were included in this study. We considered the first posttreatment MR imaging scan, irrespective of whether it was the baseline scan or preceded by CECT with or without PET. We excluded patients with inadequate clinical or imaging follow-up or who had missing data, NI-RADS 4 with confirmed recurrence before scanning, non-contrast-enhanced scans, and scans with low-quality images that showed remarkable artifacts.

An initial search in the PACS revealed that 335 CEMRI neck scans were performed for 221 patients between June 2018 and September 2020, of whom 87 patients had HNSCC. We excluded 15 patients because of inadequate histopathologic data or follow-up, 2 patients because of lack of postcontrast sequences, and 1 patient because of profound artifacts from an inserted maxillary prosthesis.

### Image Acquisition

Images were acquired with a 1.5T scanner (Ingenia, Philips Healthcare) using a 16-channel neurovascular coil. Imaging started from the skull base to the thoracic inlet, with FOV anterior to posterior 230 mm, and 4-mm section thickness with no gap. Axial single-shot SE EPI DWI was acquired ( $b = 0$  and 800 seconds/mm<sup>2</sup>, TR/TE 2920/67 ms, section thickness 4 mm, and voxel size 3.2 × 2.6 × 4.0 mm). ADC was automatically generated by the implemented software, including precontrast axial SE T1WI (TE/TR: 21/633 ms), coronal SE T1 (TE/TR: 14/555 ms), axial SE T2WI (TE/TR: 10/7039 ms), sagittal SE T2WI (TE/TR: 100/3196.7 ms), and coronal T2 STIR (TR/TI = 3500/150, TE = 80 ms). A gadolinium-based contrast agent (dimeglumine gadopentetate) (0.1 mmol/kg) was administered using an injector with a flow rate of 2–3 mL/s followed by postcontrast T1WI with fat saturation, in the axial (TR/TE: 611/21 ms), sagittal (TR/TE: 570/14 ms), and coronal (TR/TE: 570/14 ms) planes.

### Image Analysis and Applied Diagnostic Criteria

Data were transferred to an IntelliSpace Portal 9.0 workstation (Philips Healthcare). Scans were interpreted by 2 neuroradiologists with different levels of experience (5 and 15 years) in head and neck imaging, both of whom have been trained on NI-RADS

reporting at our institution. NI-RADS has been the reporting template in use for posttreatment of HNSCC cases since early 2018 according to the ACR NI-RADS lexicon and the directions published in the Aiken and Hudgins<sup>5</sup> guide article and the white paper of the ACR NI-RADS committee.<sup>1</sup> Readers had access to patients' demographic data (names and identification numbers had been anonymized), the therapeutic history, the pretreatment scans, and any other preceding posttreatment CECT with or without PET scan and were blinded to the clinical or pathologic outcome. Discrepant interpretations were resolved by consensus.

Three polygonal ROIs were inserted manually by the neuroradiologist with 5 years' experience on  $b = 800$  images either on the same or consecutive axial sections, according to the size and extent of the primary targets and copied automatically on the corresponding ADC maps. ROIs were placed on the most enhancing parts in the presence of enhancement, excluding necrotic areas guided by contrast-enhanced-T1WI and T2WI in the same axial sections. The average ADC<sub>mean</sub> value for the 3 measurements was estimated for all targets.

Two reporting template forms were used to evaluate primary targets, including the primary tumor site and any regional non-nodal target as associated perineural tumor spread; 1 was template confined to the existing NI-RADS lexicon and scoring system,<sup>1,5</sup> and the final score was provided according to the higher numeric scoring lesion in case of more than 1 primary target. The other template included the diffusion criteria in qualitative and quantitative forms and T2 SI of primary targets, and scoring was performed according to our modified rules to the current NI-RADS lexicon.

Based on the available literature<sup>6,8</sup> and the authors' experience, a defined scale for T2 SI evaluation was set: 1) isointense SI to the normal-appearing surrounding tissues, 2) very dark T2 SI (much lower than original tumor and muscle) (Figs 1A and 2A), 3) intermediate T2 SI (similar to the initial tumor signal), (Fig 1A), and 4) high T2 SI for tissues displaying SI between muscle SI and fluid, or much higher than the original tumor. Correlation with the pretreatment tumor signal was performed for 56 cases with available pretreatment CEMRI.

For diffusion criteria, the scale used for visual interpretation of the signal to determine whether it was high or low was compared with the brain stem signal in ADC maps as follows: 1) diffusion restriction for low signal in the ADC map compared with the brain stem signal with high signal in DWI corresponding to abnormal enhancement (Fig 1C) and/or similar to the original tumor signal; and 2) facilitated diffusion for high signal in the ADC map compared with the brain stem with high or low signal on DWI (Figs 1D and 2C) or higher than the original tumor signal.

### Image Analysis Using T2 SI and DWI as Modified Rules for NI-RADS Categories

We incorporated diffusion features and T2 SI into NI-RADS as modified rules. The presence of both diffusion restriction and intermediate T2 SI would upgrade the NI-RADS categories by 1 grade (from categories 1 to 2 and 2 to 3). Conversely, the absence of both would downgrade NI-RADS categories by 1 grade (Fig 2) (from categories 3 to 2 and 2 to 1). The presence of only 1 feature without the other feature would not alter the original NI-RADS risk category.

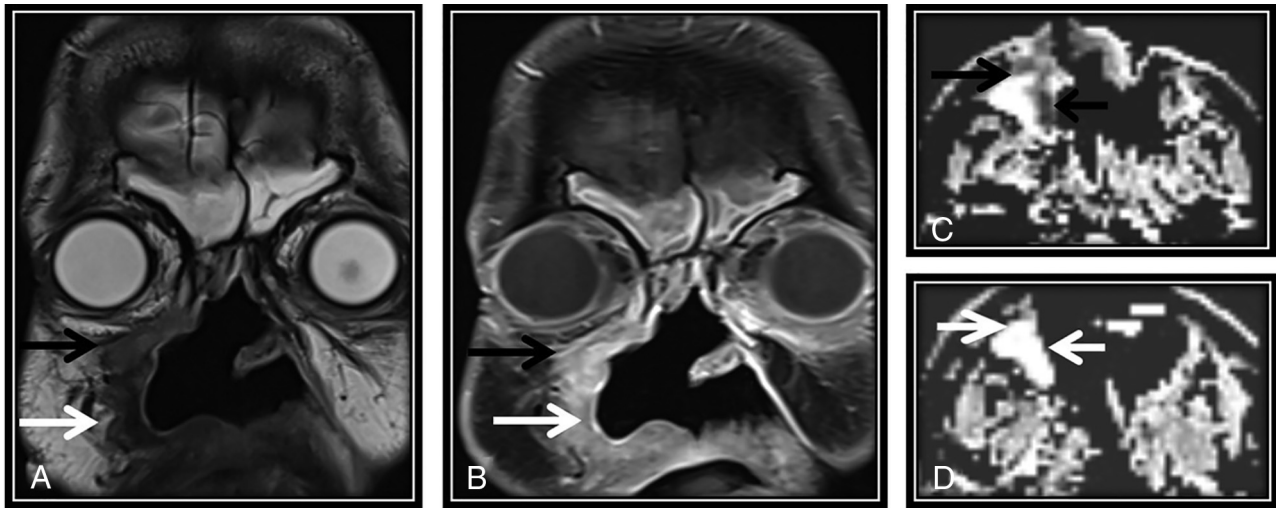


**FIG 1.** Concordance between NI-RADS category, T2 SI, and DWIs is demonstrated in this posttreatment MR imaging surveillance scan done after surgery and RTH for sinonasal squamous cell carcinoma. Coronal T2WI (A) and coronal contrast-enhanced T1WI (B) show a surgical bed discrete nodule (black arrow) that displays intermediate T2 SI (A) and postcontrast enhancement (B), fulfilling NI-RADS 3 and confirmed to be squamous cell carcinoma by histopathology. C, Axial ADC map of the surgical bed shows a corresponding low-ADC signal (black arrow). White arrows point to circumferential soft tissue thickening with sheetlike enhancement (B), which shows low T2 SI (A), absent diffusion restriction (D), and was confirmed to be posttreatment fibrous tissue.



**FIG 2.** The first post-CRTH MR imaging follow-up for a known case of nasopharyngeal carcinoma with perineural tumor spread (PNTS) showing discordant findings between NI-RADS category, T2 SI, and DWI. There is a clear primary tumor site at the nasopharynx (not demonstrated here), yet a regional non-nodal target was noted. A, Axial T2WI shows orbital apex dark T2 SI tissue keeping with fibrotic scarring (arrow). B, This lesion shows discrete postcontrast enhancement (arrow) (secondary to PNTS along the ophthalmic nerve) categorized as NI-RADS 3. C, Axial ADC map of the surgical bed shows a corresponding facilitated diffusion (arrow). According to our proposed modifying rules, downgrading to category 2 was done. Follow-up by PET/CT showed no FDG uptake (not demonstrated here) that was confirmed to be post-RTH fibrotic scarring by further follow-up. Note the right temporal lobe after RTH injury.

### Standard of Reference

Criteria for negative disease included negative clinical and MR imaging follow-up performed after 12 months or negative biopsy results. Criteria for LTR included positive biopsy results, evident tumor on clinical examination, or evidence of disease progression on subsequent follow-up scans as determined by the Response Evaluation Criteria in Solid Tumors.<sup>12</sup>

### Ethics Approval

All procedures performed in the study were in accordance with the ethical standards of the institutional research committee and with the 1964 Helsinki Declaration and its later amendments. For this type of study informed consent was not required and waived by the ethical committee.

### Statistical Analysis

The collected data were revised, coded, and tabulated using SPSS 20 (IBM). For descriptive statistics, the mean, SD, and range were used for numerical data; frequency and percentage were used for non-numeric data. For analytical statistics, the Student *t* test was used to assess the statistical significance of the difference in  $ADC_{mean}$  values between LTR and benign lesions. ROC curve analysis of  $ADC_{mean}$  values was performed according to the standard of reference. The diagnostic performance of ACR NI-RADS, DWI in its qualitative and quantitative forms, T2 SI, and NI-RADS combined with T2 SI and DWI were assessed in terms of sensitivity, specificity, positive predictive value (PPV), negative predictive value (NPV), and accuracy. Kappa statistics were used to compute the measure of agreement.

between 2 investigational methods, with values of 0.2–0.4 indicating fair agreement; 0.41–0.6, moderate agreement; 0.61–0.8, substantial agreement; and 0.8–1.0, almost perfect agreement.  $P < .05$  was considered significant.

## RESULTS

### Patients and Tumor Characteristics

The study population consisted of 69 patients: 41 males (59.4%) and 28 females (40.6%), with the mean age of  $50.55 \pm 16.82$  (range, 18–85 years). Twenty-two (31.9%) patients underwent surgical excision and received radiation therapy (RTH), 19 (27.5%) received chemoradiation therapy (CRTH), 12 (17.4%) underwent surgery only, 9 (13.0%) underwent surgery combined with CRTH, and 7 (10.1%) received RTH. Table 1 demonstrates the tumor demographics and scan order.

### Descriptive Statistics for LTR and Benign Posttreatment Lesions

Pathology or follow-up confirmed diagnosis in 26/69 (37.7%) patients, and imaging follow-up confirmed diagnosis in 43/69 (62.3%) patients. LTR occurred in 26/69 (37.7%) patients.

### Results of Image Interpretation and Applied Diagnostic Criteria Relative to the Standard of Reference

The results of the imaging analysis of the primary targets and the results of the diagnostic performance of T2 SI, DWI (qualitative and quantitative), NI-RADS, and NI-RADS rescoring, for the detection of LTR for the primary targets, are listed in Table 2 and 3.

For diffusion criteria, there was no statistically significant difference between the qualitative and quantitative assessment of DWI, with 28/69 lesions (40.6%) showing diffusion restriction with a low ADC signal; 24/28 were LTR, and 4/28 were post-treatment changes. A total of 41/69 lesions (59.4%) demonstrated no diffusion restriction, 39/41 showed no recurrence, and 2/41 had LTR.

The mean ADC value for LTR was  $0.94 \pm 0.38$ , and the mean ADC value

**Table 1: Tumor characteristics and scan order of the included population**

		Patients (n)	Patients (%)
Subsite	Larynx	12	17.4
	Oral cavity and oropharynx	25	36.2
	Hypopharynx	2	2.9
	Sinonasal	10	14.5
	Skull base	1	1.4
	Nasopharynx	13	18.8
Pathologic grade	Salivary	6	8.7
	Low	14	20.3
	Moderate	37	53.6
Tumor stage <sup>a</sup>	High	18	26.1
	Tis	1	1.4
	T1	7	10.14
	T2	24	34.8
	T3	22	31.9
	T4	15	21.7
Scan order	First follow-up	54	78.3
	Second follow-up	8	10.1
	Third follow-up	8	11.6

**Note:**—Tis indicates carcinoma in situ.

<sup>a</sup> American Joint Committee on Cancer.<sup>20</sup>

**Table 2: Results of image analysis by T2 SI, DWI (qualitative and quantitative), NI-RADS, and NI-RADS rescoring for the primary targets**

			Standard of Reference	
			Negative n (%)	Positive n (%)
NI-RADS	NI-RADS 1		20 (46.51)	1 (3.85)
	NI-RADS 2		15 (34.88)	3 (11.54)
	NI-RADS 3		8 (18.6)	22 (84.62)
T2 SI	Isointense to surrounding tissue		4 (9.3)	1 (3.85)
	Dark		15 (34.88)	1 (3.85)
	Intermediate		5 (11.63)	24 (92.31)
DWI	High		19 (44.19)	0 (0)
	Facilitated		39 (90.7)	2 (7.69)
	Restricted		4 (9.3)	24 (92.31)
NI-RADS combined with T2 and DWI	NI-RADS 1		30 (69.77)	1 (3.85)
	NI-RADS 2		10 (23.26)	2 (7.69)
	NI-RADS 3		3 (6.98)	23 (88.46)

**Table 3: Diagnostic performance of T2 SI, DWI (qualitative and quantitative), NI-RADS, and NI-RADS rescoring for the detection of LTR for the primary targets**

	T2 SI	DWI with ADC $\leq 1.3$	NI-RADS	NI-RADS-DWI-T2 SI
TP (n)	24	24	22	23
TN (n)	38	39	35	40
FP (n)	5	4	8	3
FN (n)	2	2	4	3
Sensitivity (%) (95% CI)	92.31 (74.87–99.05)	92.3 (74.87–99.05)	84.62 (65.13–95.64)	88.46 (69.85–97.55)
Specificity (%) (95% CI)	88.37 (74.92–96.11)	90.7 (77.86–97.41)	81.4 (66.60–91.61)	93.02 (80.94–98.54)
PPV (%) (95% CI)	82.76 (67.64–91.68)	85.71 (70.10–93.89)	73.33 (59.03–84.00)	88.46 (71.84–95.84)
NPV (%) (95% CI)	95.00 (83.32–98.64)	95.12 (83.69–98.67)	89.74 (77.84–95.61)	93.02 (82.10–97.49)
Accuracy (%) (95% CI)	89.86 (80.21–95.82)	91.30 (82.03–96.74)	82.61 (71.59–90.68)	91.30 (82.03–96.74)

**Note:**—TP indicates true-positive; TN, true-negative.



**Table 4: Agreement between DWI (qualitative and quantitative), T2 SI, NI-RADS, and NI-RADS combined with DWI and T2 SI for the primary targets and the standard of reference**

		Standard of Reference		Agreement		
		Negative n (%)	Positive n (%)	Kappa	95% CI	P Value
DWI	Restricted	4 (9.3)	24 (92.31)	0.818	0.68–0.96	<.001
	Facilitated	39 (90.7)	2 (7.69)			
T2 SI	Intermediate	5 (11.63)	24 (92.3)	0.789	0.64–0.94	<.001
	No abnormality; low or high SI	38 (88.37)	2 (7.69)			
NI-RADS combined with T2 and DWI	Category 3	3 (6.98)	23 (88.46)	0.815	0.67–0.96	<.001
	Categories 1 and 2	40 (93.02)	3 (11.54)			
NI-RADS	Category 3	8 (18.6)	22 (84.62)	0.641	0.46–0.82	<.001
	Categories 1 and 2	35 (81.4)	4 (15.38)			

for benign posttreatment changes was  $1.98 \pm 0.55$  ( $P < .001$ ).

ROC curve analysis showed an AUC of 0.945 (0.875–0.990 CI), with cutoff  $ADC_{mean} \leq 1.3 \times 10^{-3} \text{ mm}^2/\text{s}$ , which showed the highest sensitivity, specificity, PPV, and NPV (92.31%, 90.7%, 85.7%, and 95.1%, respectively).

For T2 SI, 29/69 lesions showed intermediate T2 SI, 24/29 were LTR, and 5/29 lesions were posttreatment benign changes. A total of 40 lesions demonstrated no abnormality, low or high SI in T2WI, 38/40 showed no recurrence, and 2/40 showed LTR.

Regarding NI-RADS, 39/69 targets were categorized as NI-RADS 1 ( $n = 21$ ) or 2 ( $n = 18$ ), 35/39 were found to be negative, and 4 lesions were LTR; 30 lesions were categorized as NI-RADS 3, 22/30 lesions proved to be LTR, and 8 lesions were negative according to the criterion standard.

After inclusion of T2 SI and DWI as modifying rules to NI-RADS categories, 7 NI-RADS category 3 targets were downgraded to category 2, 3 NI-RADS 2 targets were upgraded to category 3, and 10 NI-RADS 2 targets were downgraded to NI-RADS 1.

Agreement between DWI, T2 SI, NI-RADS, and NI-RADS combined with DWI and T2 SI of the primary targets, and the standard of reference is shown in Table 4.

## DISCUSSION

In the current study, incorporation of T2 SI and diffusion features into NI-RADS as modifying rules showed high diagnostic performance, with higher sensitivity, specificity, PPV, and NPV of 88.46%, 93.02%, 88.46%, and 93.02%, respectively, compared with the current ACR NI-RADS template, which showed a sensitivity, specificity, PPV, and NPV of 84.62%, 81.40%, 73.33%, and 89.74%, respectively, with the difference being more notable in specificity than in sensitivity.

Several previous studies evaluated the utility of DWI in differentiating posttreatment changes from recurrence and concluded that DWI showed high diagnostic performance.<sup>7,11,13–16</sup> Morphologic imaging features for LTR described in previous literature included infiltrative mass appearance, with intermediate to high SI in T2 WIs and postcontrast enhancement. However, these features could overlap with those of benign posttreatment findings such as posttherapy inflammation and fibrosis.<sup>13,16</sup> Therefore, dependence on only morphologic features could result in increased false-positive (FP) cases. The current ACR NI-RADS lexicon was developed for CECT with or without PET; thus, it does not include MR imaging-specific sequences. We suggest the addition of T2 SI and diffusion

features to the current lexicon to adapt it to posttreatment surveillance with CEMRI, taking advantage of its routine use in daily practice.

In the available literature, the performance of NI-RADS was assessed for CECT with or without PET at different time points in terms of discrimination between categories.<sup>4</sup> Two other studies investigated the predictive value of the first posttreatment PET/CT using NI-RADS.<sup>3,17</sup> Wangaryattawanich et al<sup>18</sup> investigated the PPV of NI-RADS categories 3 and 4 for PET/CT and concluded that NI-RADS 3 and 4 have a PPV of 56% and 100%, respectively. Our results showed a higher PPV and lower NPV for NI-RADS compared with the previous studies. This could be attributable to the inherent difference between the performance of CEMRI and contrast-enhanced PET/CT in posttreatment imaging surveillance, as also supported by the results of Kreiger et al,<sup>4</sup> which showed a much higher rate of true-positive disease with the use of CECT (91.7%) compared with PET/CT (40%).

In this study, we assessed the T2 SI and diffusion features of the primary targets; both showed high diagnostic performance relative to patient outcome. Comparing the diagnostic performance of T2 SI and DWI and combining both with NI-RADS showed that DWI had a higher specificity and accuracy of 90.70% and 91.30%, respectively, compared with 88.37% and 89.86%, respectively, for T2 SI; both showed similar sensitivities of 92.31%. Incorporating T2 SI and DWI within the NI-RADS yielded higher specificity (93.02%) and higher PPV compared with either T2 SI or DWI alone, and accuracy (91.30%) similar to the diffusion criteria. The kappa coefficient for the concordance between NI-RADS scoring of the primary tumor site and the outcome was 0.641, and higher agreement (0.815) was obtained by combining DWI and T2 SI with NI-RADS scoring.

Ailianou et al<sup>6</sup> concluded that morphologic MR imaging with defined criteria had a similar diagnostic performance to DWI, with the combination of both yielding higher results. Precise analysis of signal intensities on morphologic MR imaging increased the specificity of DWI, whereas the overall effect on sensitivity was less pronounced. The results of the current study are concordant with those of Ailianou et al<sup>6</sup> regarding the higher sensitivity and specificity obtained after incorporation of DWI into NI-RADS morphologic features, with a more pronounced effect on specificity than sensitivity.

The current study showed an optimal  $ADC_{mean}$  threshold of  $1.3 \times 10^{-3} \text{ mm}^2/\text{s}$  to discriminate between benign changes and

LTR with a sensitivity, specificity, and accuracy of 92.31%, 90.70%, and 91.30%, respectively. This agrees with Jajodia et al,<sup>10</sup> who showed the same ADC threshold with a sensitivity, specificity, and accuracy of 94%, 83.3%, and 93.6%, respectively. Minor differences in diagnostic parameters could be due to the different characteristics of the included population; for example, they included patients with lesions >5 mm, presenting between 3 months and 2 years, whereas we included scans performed within the first year after treatment with no specific size criteria for lesions for inclusion.

In our study, analysis of T2 SI performance individually revealed 2 false-negative (FN) and 5 FP cases; 1 of the FN cases was a pathologically proved residual tongue squamous cell carcinoma. The residual tumor was not detected during the first post-treatment MR imaging scan, including DWI, T2, and the NI-RADS system. This could be explained by the presence of microscopic residual tumor cells in the initial study beyond MR imaging resolution because the discrete enhancing lesion became apparent on the follow-up scans. The second FN case was a case with a primary target lesion with low T2 SI that resembled fibrotic tissue; it was proved pathologically to contain a small 6-mm residual tumor, suggesting that tiny residual tumors may exist within a sizable fibrotic tissue, for which follow-up would be useful.

Five FP cases by T2 SI corresponded to posttreatment fibrotic scarring, suggesting that fibrotic tissue may present with intermediate SI in the early posttreatment phase.

Two FN and 4 FP cases were identified by DWI; the FN results in DWI are explained by either microscopic tumor tissue or the presence of posttreatment edema or inflammation in the early posttreatment scans. The FP results with DWI were attributed to lymphoid hyperplasia and early stages of fibrosis that may show diffusion restriction, which requires further follow-up.

Adding DWI and T2 signal features helped in reducing the number of FP findings caused by NI-RADS 3 criteria because of the enhancement associated with posttreatment benign findings that can present as masslike lesions.<sup>16</sup> Although our results showed a very comparable diagnostic performance between DWI (quantitative and qualitative forms) alone and the combined criteria, further studies on a larger scale are required to confirm these results. Taking into consideration the limitations of dependence on diffusion and ADC values with related motion and susceptibility artifacts, variations in ADC values using different MR imaging scanners and different b-values, and the lack of a definite cutoff value for ADC,<sup>7,13,19</sup> we recommend incorporating diffusion criteria and T2 SI into the NI-RADS system to benefit from combined functional, morphologic, and enhancement features and to overcome the intrinsic limitations of each of them when used individually.

### Limitations of the Study

One limitation of our study is that it is a retrospective, single-center study. Hence, minor variations in scan timing occurred. Further multicenter studies with larger sample volumes are required to support these results.

### CONCLUSIONS

Incorporation of diffusion criteria and T2 SI into the current NI-RADS criteria for primary tumor site assessment as modifying

rules enhanced the diagnostic validity and accuracy of the ACR NI-RADS template.

### REFERENCES

1. Aiken AH, Rath TJ, Anzai Y, et al. **ACR Neck Imaging Reporting and Data Systems (NI-RADS): a white paper of the ACR NI-RADS Committee.** *J Am Coll Radiol* 2018;15:1097–08 [CrossRef Medline](#)
2. Aiken AA, Farley A, Baugnon KL, et al. **Implementation of a novel surveillance template for head and neck cancer: Neck Imaging Reporting and Data System (NI-RADS).** *J Am Coll Radiol* 2016;13:743–46 [CrossRef Medline](#)
3. Wangyattawanich P, Branstetter BF, Hughes M, et al. **Negative predictive value of NI-RADS category 2 in the first posttreatment FDG-PET/CT in head and neck squamous cell carcinoma.** *AJNR Am J Neuroradiol* 2018;39:1884–88 [CrossRef Medline](#)
4. Krieger DA, Hudgins PA, Nayak GK, et al. **Initial performance of NI-RADS to predict residual or recurrent head and neck squamous cell carcinoma.** *AJNR Am J Neuroradiol* 2017;38:1193–99 [CrossRef Medline](#)
5. Aiken AH, Hudgins PA. **Neck Imaging Reporting and Data System.** *Magn Reson Imaging Clin N Am* 2018;26:51–62 [CrossRef Medline](#)
6. Ailianou A, Mundada P, De Perrot T, et al. **MRI with DWI for the detection of posttreatment head and neck squamous cell carcinoma: why morphologic MRI criteria matter.** *AJNR Am J Neuroradiol* 2018;39:748–55 [CrossRef Medline](#)
7. Vaid S, Chandorkar A, Atre A, et al. **Differentiating recurrent tumours from post-treatment changes in head and neck cancers: does diffusion-weighted MRI solve the eternal dilemma?** *Clin Radiol* 2017;72:74–83 [CrossRef Medline](#)
8. King AD, Keung CK, Yu KH, et al. **T2-weighted MR imaging early after chemoradiotherapy to evaluate treatment response in head and neck squamous cell carcinoma.** *AJNR Am J Neuroradiol* 2013;34:1237–41 [CrossRef Medline](#)
9. Becker M, Varoquaux D, Combescure C, et al. **Local recurrence of squamous cell carcinoma of the head and neck after radio (chemo)therapy: diagnostic performance of FDG-PET/MRI with diffusion-weighted sequences.** *Eur Radiol* 2018;28:651–63 [CrossRef Medline](#)
10. Jajodia A, Aggarwal D, Chaturvedi AK, et al. **Value of diffusion MR imaging in differentiation of recurrent head and neck malignancies from post treatment changes.** *Oral Oncol* 2019;96:89–96 [CrossRef Medline](#)
11. Connolly M, Srinivasan A. **Diffusion-weighted imaging in head and neck cancer: technique, limitations, and applications.** *Magn Reson Imaging Clin N Am* 2018;26:121–33 [CrossRef Medline](#)
12. Eisenhauer EA, Therasse P, Bogaerts J, et al. **New response evaluation criteria in solid tumours: revised RECIST guideline (version 1.1).** *Eur J Cancer* 2009;45:228–47 [CrossRef Medline](#)
13. Tshering Vogel DW, Zbaeren P, Geretschlaeger A, et al. **Diffusion-weighted MR imaging including bi-exponential fitting for the detection of recurrent or residual tumour after (chemo)radiotherapy for laryngeal and hypopharyngeal cancers.** *Eur Radiol* 2013;23:562–69 [CrossRef Medline](#)
14. Zhou Q, Zeng F, Ding Y, et al. **Meta-analysis of diffusion-weighted imaging for predicting locoregional failure of chemoradiotherapy in patients with head and neck squamous cell carcinoma.** *Mol Clin Oncol* 2018;8:197–203 [CrossRef Medline](#)
15. Fujima N, Yoshida D, Sakashita T, et al. **Residual tumour detection in post-treatment granulation tissue by using advanced diffusion models in head and neck squamous cell carcinoma patients.** *Eur J Radiol* 2017;90:14–19 [CrossRef Medline](#)
16. Abdel Razek AAK, Kandeel AY, Soliman N, et al. **Role of diffusion-weighted echo-planar MR imaging in differentiation of residual or recurrent head and neck tumors and posttreatment changes.** *AJNR Am J Neuroradiol* 2007;28:1146–52 [CrossRef Medline](#)

17. Hsu D, Chokshi FH, Hudgins PA, et al. **Predictive value of first post-treatment imaging using standardized reporting in head and neck cancer.** *Otolaryngol Head Neck Surg* 2019;161:978–85 [CrossRef Medline](#)
18. Wangyattawanich P, Branstetter BF, Ly JD, et al. **Positive predictive value of neck imaging reporting and data system categories 3 and 4 post treatment FDG-PET/CT in head and neck squamous cell carcinoma.** *AJNR Am J Neuroradiol* 2020;41:1070–75 [CrossRef Medline](#)
19. Chung SR, Choi YJ, Suh CH, et al. **Diffusion-weighted magnetic resonance imaging for predicting response to chemoradiation therapy for head and neck squamous cell carcinoma: a systematic review.** *Korean J Radiol* 2019;20:649–61 [CrossRef Medline](#)
20. Amin MB, Edge SB, Greene FL, et al. *AJCC Cancer Staging Manual.* Springer; 2017.